

## Magnetic properties of finite antiferromagnetic superlattices: Statics, dynamics, and the surface spin-flop phase

R. W. Wang and D. L. Mills

Department of Physics, University of California, Irvine, California 92717

(Received 31 January 1994)

We use the numerical self-consistent mean-field method to examine the ground-state configurations of finite-size multilayers constructed from ferromagnetic films which are antiferromagnetically coupled. At intermediate fields, a surface spin-flop state, as suggested by Keffer and Chow, has been found for even numbered multilayers, but not for odd numbered ones. These are confirmed by experimental observations on systems such as Fe/Cr. A simple macroscopic approach has been devised in calculating the spin-wave excitations for the various field-induced ground states. Special emphasis is placed on the influence of interfilm dipolar couplings on the spin-wave spectrum. We note, for example, that there are substantial differences for the two cases  $k_{\parallel}D \ll 1$  and  $k_{\parallel}D \gtrsim 1$ , with  $D$  the thickness of the finite superlattice, and  $k_{\parallel}$  the wave vector of the spin waves parallel to its surface.

### I. INTRODUCTION

It is now possible to synthesize magnetic superlattice structures from diverse constituents. The resulting materials can display unique properties not realized in conventional bulk crystalline magnets. An example is provided by the phenomenon of giant magnetoresistance, reported first in Fe/Cr superlattices by Fert and co-workers.<sup>1</sup>

In this paper, we explore the theory of the static magnetic structure and spin dynamics realized in a very interesting superlattice structure synthesized recently at Argonne National Laboratory, by Fullerton and his colleagues.<sup>2</sup> These are also Fe/Cr superlattices, but are grown on a MgO(110) substrate. The exchange coupling mediated by the Cr layers can be either ferromagnetic or antiferromagnetic in nature, depending on the Cr thickness, very much as in the samples explored in Ref. 1. The new feature here is the presence of a twofold in-plane anisotropy, present by virtue of the imprint provided by the MgO(110) substrate. We show here that the anisotropy, in combination with the interfilm exchange, endows these superlattices with a particularly rich magnetic phase diagram. This is the case when the interfilm coupling is antiferromagnetic in the superlattice. Indeed, the materials allow one to explore a phenomenon discussed in the theoretical literature on antiferromagnetism over two decades ago: the surface spin-flop transition.<sup>3,4</sup> Our calculations show that, for a finite structure, the state realized is richer in physical content than realized by the early authors. We comment briefly on the earlier literature before we proceed.

Much of our understanding of antiferromagnetism in bulk crystals comes from the study of the classical two-sublattice antiferromagnet  $\text{MnF}_2$ , or closely related compounds. The magnetic structure of  $\text{MnF}_2$ , below its Néel temperature and in zero external magnetic field, is illustrated in Fig. 1(a). One has two interpenetrating magnetic sublattices, one directed along  $+\hat{z}$ , and one along  $-\hat{z}$ .

The structure is stabilized by a twofold anisotropy (of dipolar origin), which makes  $\hat{z}$  an easy direction. Application of a magnetic field parallel to  $\hat{z}$  can induce a first-order phase transition to the spin-flop phase,<sup>5</sup> in which each sublattice is canted with respect to  $\hat{z}$ , as illustrated schematically in Fig. 1(b).

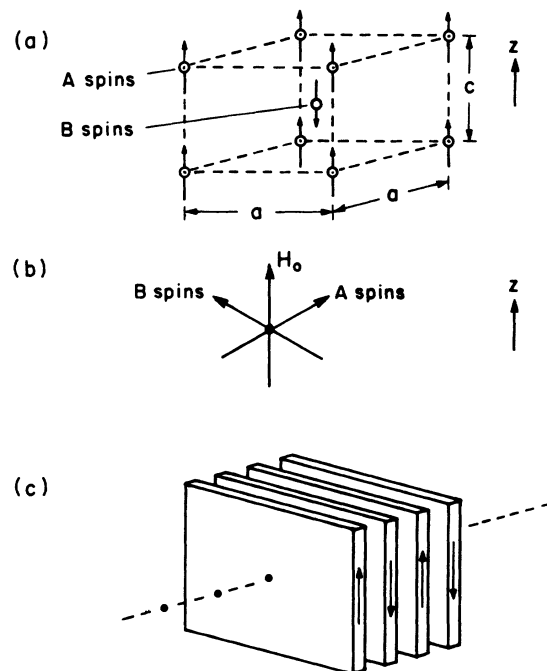


FIG. 1. (a) Magnetic structure of the antiferromagnet  $\text{MnF}_2$ , illustrating the  $A$  and  $B$  spin sublattices. (b) Orientation of the  $A$  and  $B$  total sublattice magnetic moments, when the external magnetic field  $H_0$  is strong enough to drive the system into the spin-flop phase. (c) The low-field state of the Fe/Cr superlattice, when the interfilm coupling is antiferromagnetic in character. Each Fe film may be viewed as a ferromagnetic spin sheet exchange coupled to neighboring spin sheets, very much as in the case for the (100) planes of spins in (a).

In the theoretical literature some years ago, the influence of a surface on the properties of such material was explored. For example, Saslow and Mills<sup>3</sup> examined the low-temperature properties of a  $\text{MnF}_2$ -type antiferromagnet with a (100) surface. They found a surface spin wave, which in the long-wavelength limit lies within the frequency gap below the lowest bulk antiferromagnetic spin-wave frequency. The (100) planes of spins in the  $\text{MnF}_2$  structure form ferromagnetically coupled spin sheets, notice. It was found that application of a magnetic field antiparallel to the surface moments drives the surface spin wave "soft," at a field well below that required to generate the bulk spin-flop transition: this implies the system must undergo a surface spin-flop transition at the field where the surface wave softens.

Mills presented a theoretical description of the surface spin-flop phase,<sup>4</sup> which was later modified importantly by Keffer and Chow.<sup>6</sup> These authors noted that additional terms must be retained in the analysis, and these modify the earlier picture. Keffer and Chow concluded that, in the semi-infinite antiferromagnet, the bulk spin-flop phase is nucleated on the surface. According to their analysis, one realizes the surface instability at the critical field discussed earlier,<sup>3,4</sup> but with increasing field, the surface phase expands in depth, to envelope the entire crystal at the bulk spin-flop field. Very near the end of their paper, in brief comments, Keffer and Chow<sup>6</sup> discussed the nature of the surface instability in an antiferromagnet with a finite number of (100) spin planes. The calculations presented here confirm the striking picture envisioned in these terse comments, and in fact show the surface spin-flop phase of the finite structure to be much richer than envisioned by Keffer and Chow.

There were unsuccessful attempts to verify the predictions just discussed, on the surface of antiferromagnets of the  $\text{MnF}_2$  type.<sup>7</sup> For such attempts to be successful, the demands on surface quality are severe. For example, both the surface spin wave described by Saslow and Mills, along with the surface spin-flop phase (at fields in the near vicinity of the surface spin-flop transition), were predicted to be confined to the outmost ten atomic layers or so.

The Fe/Cr structures grown on MgO(110) are isomorphic to the  $\text{MnF}_2$  antiferromagnets with a (100) surface. We have sheets of ferromagnetically coupled spins in planes parallel to the surface, with antiferromagnetic coupling between planes; there is a twofold anisotropy axis in plane. Recent experiments have explored magnetization curves of finite Fe/Cr superlattices, and have uncovered clear and unambiguous evidence for the surface spin-flop transition.<sup>8</sup> The purpose of this paper is to discuss the theory of the spin configuration realized in these materials, as a function of an externally applied magnetic field. We also present the theory of the collective spin waves in such structures. It should be remarked that a brief discussion of some of these results has been presented elsewhere.<sup>8</sup>

This paper is organized as follows. In Sec. II, we discuss the spin configuration realized by the finite superlattice, in a spatially uniform external magnetic field. Included in the section is a description of the hysteresis

loops associated with these systems. Section III discusses the collective spin-wave excitations of the superlattice structure. Here (dipolar) magnetic fields generated by the spin motions are an important source of interfilm coupling, as in earlier studies. We describe a simple means of including these couplings, in the limit that the ferromagnetic films in the superlattice are very thin.

## II. THE INFLUENCE OF A MAGNETIC FIELD ON THE SUPERLATTICE STRUCTURE

We consider a finite superlattice of ferromagnetic films, with antiferromagnetic interfilm coupling of strength  $H_E$ , so that in zero magnetic field we realize the ground state illustrated in Fig. 1(c). The film magnetizations here are aligned along an easy axis in the plane, present in the structures that motivated the analysis described here by virtue of their growth on the MgO(110) substrate.

Application of a sufficiently strong magnetic field will initiate spin canting, and the angle between the magnetization of the  $l$ th film and the magnetic field  $H_0$  will be denoted by  $\alpha_l$ . While the magnetization of each film will be canted away from the easy axis, reminiscent of the spin-flop phase in bulk antiferromagnets, it will very clearly be confined to the plane of the film. If the magnetization is tilted out of plane, to acquire a component  $\mathbf{M}_\perp$  normal to the film surfaces, elementary magnetostatics informs one that an internal demagnetizing field  $-4\pi\mathbf{M}_\perp$  antiparallel to  $\mathbf{M}_\perp$  itself must be present. Clearly, in this circumstance, the magnetization of each film lies in plane.

The energies of the system are then controlled by the interfilm exchange coupling, the anisotropy, and the external magnetic field. For the example we have in mind, the intrafilm exchange coupling is so strong that all moments within a given film are locked rigidly into a ferromagnetic array. In magnetic-field units, we write the energy of the system, suitably normalized, in the form

$$E = \frac{H_E}{2} \sum_{l=1}^{N-1} \cos(\alpha_l + \alpha_{l+1}) - \frac{H_A}{2} \sum_{l=1}^N \cos^2 \alpha_l - H_0 \sum_{l=1}^N \cos \alpha_l. \quad (1)$$

The angle convention used here is illustrated in Fig. 2. Note that  $\alpha_1$  is positive when film 1 is canted towards the  $+\hat{x}$  direction, while  $\alpha_2$  is positive when film 2 is canted towards the  $-\hat{x}$  direction. The convention on the parameters in Eq. (1) is the following. If all terms are multiplied by  $f_1 M_s$ , with  $M_s$  the saturation magnetization of each ferromagnetic film and  $f_1$  the fraction of the superlattice's volume occupied by the ferromagnetic constituents, then we have the energy per unit volume associated with the magnetic interactions. In magnetic-field units,  $H_E$  is the effective field experienced by a given film, when both its neighbors are in the antiferromagnetic state, where all differences  $\alpha_l - \alpha_{l\pm 1}$  equal  $\pi$ .

$$H_E [(1 - \delta_{l,1}) \sin(\alpha_{l-1} + \alpha_l) + (1 - \delta_{l,N}) \sin(\alpha_{l+1} + \alpha_l)] = H_A \sin 2\alpha_l + 2H_0 \sin \alpha_l, \quad (2)$$

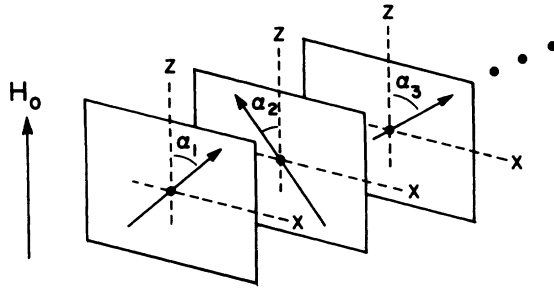


FIG. 2. Arrangement of magnetic moments in the finite superlattice, in the canted state. This illustrates the conventions used in Sec. II.

and verify that the solution is in fact an absolute minimum of the energy.

We remark that in earlier work Nörtemann and co-workers<sup>9,10</sup> have carried out very similar analyses, for closely related materials. These authors confined their attention to the case where  $H_A=0$ , to find that in finite superlattices the presence of the two surfaces influences the moment distribution significantly. We agree, of course, and argue that the presence of the twofold anisotropy makes the magnetic phase diagram very rich, for reasons discussed in Sec. I.

To appreciate this point, consider a finite superlattice with  $N$  ferromagnetic films. If  $N$  is odd, and the sample is placed in a weak external field, the state of lowest energy will be an antiferromagnetic arrangement of the film magnetizations. The two end films have magnetizations parallel to each other, and also parallel to the external field. As the field is increased, a spin-flop transition is induced. In the spin-flop phase, the arrangement of the moments is as envisioned in Ref. 10; each end film is exchange coupled only to one nearest neighbor, whereas the interior films are each coupled to two neighbors. The end films are thus more closely aligned with the external field than those in the interior of the structure. The end effects also lower the field required to enter the flop phase.

If  $N$  is even, the situation is very different. Now the magnetic moments of the end films are necessarily antiparallel; one of the two is thus antiparallel to the external field. This is precisely the geometry envisioned for the surface spin-flop transitions,<sup>4-6</sup> which will be induced by the external field, at a critical field well below the bulk spin-flop transition. The response characteristics of the even and odd cases are thus very different.

We first begin with a summary of our recent study of the surface spin-flop transition in the finite superlattice, and the differences between the even and the odd case. In one of the early papers, Keffer and Chow<sup>6</sup> argued that the surface spin-flop state evolves into the bulk spin-flop state in a continuous manner, though they presented no detailed calculations which describe how this occurs. We illustrate this below. It should be remarked that a brief discussion of these results has been presented elsewhere.<sup>8</sup>

We begin with a discussion of the infinitely extended structure. The antiferromagnetic ground state has all even  $\alpha_l=0$ , and all odd  $\alpha_l=\pi$ . The energy per film is

here just  $-(H_E+H_A)/2$ , independent of  $H_0$ . In the spin-flop phase,  $\alpha_l$  is independent of  $l$ , with  $\cos\alpha = H_0/(2H_E-H_A)$ . The energy per film in the spin-flop state is then  $-H_E/2 - H_0^2/2(2H_E-H_A)$ . The structure thus enters the spin-flop phase when the external field exceeds  $H_{sf}=[H_A(2H_E-H_A)]^{1/2}$ . This is a first-order, magnetic-field-induced phase transition; the system magnetization (per film) jumps discontinuously from 0, to the value  $M_s H_0/(2H_E-H_A)$ .

If the field continues to increase, there is a point where  $\cos\alpha=1$  for all films. We are then in the fully aligned ferromagnetic state. One enters the saturated state when the external field  $H_0=2H_E-H_A$ . In bulk antiferromagnets, this is a second-order phase transition.

The description of the infinitely extended superlattice just given coincides precisely with the discussion of the magnetization as a function of magnetic fields for bulk antiferromagnets,<sup>5</sup> for the case where the temperature  $T=0$  and quantum effects such as zero-point motions are ignored. In the superlattices of interest here, we are dealing with the interactions between macroscopic moments, so the classical theory is fully adequate.

Before we present our results for the finite superlattice, we comment on aspects of the numerical analysis, because uncovering some of the subtle features displayed below required demanding calculations.

One sees easily that Eq. (2) always has two trivial solutions: the antiferromagnetic configuration  $\{\alpha_{\text{odd}}=0, \alpha_{\text{even}}=\pi\}$ , and the ferromagnetic configuration  $\{\alpha_l=0, l=1, \dots, N\}$ . These are the true ground states in the low- and high-field regions, respectively.

At intermediate fields, we solve Eq. (2) for a nontrivial configuration  $\{\alpha_l, l=1, \dots, N\}$  in the same spirit as Camley and Tilley,<sup>11</sup> and also the later work of Nörtemann, Stamps and Camley.<sup>9</sup> We start with the configuration of an infinitely extended superlattice at the given field, and solve for the effective field(s) acting on each individual spin due to its neighbor(s) and then rotate the spin in such a way as to minimize its energy. This procedure is repeated until a self-consistent configuration is obtained.

As argued above, there are striking differences between superlattices with even and odd numbers of ferromagnetic layers. For  $N$  odd, we have on physical grounds the symmetry relation  $\alpha_l=\alpha_{N+1-l}$ . This applies at all fields. Hence only  $(N+1)/2$  of the spins need to be examined during each sweep. With increasing field, the antiferromagnetic ground state enters the "bulk" spin-flop state at a field  $H_{c1}$  when its energy  $-(N-1)H_E/2 - NH_A/2 - H_0$  crosses that of the latter. As the field increases, the canting angles close up, and eventually the spin-flop state merges continuously with the ferromagnetic state at a field  $H_{c2}$  slightly below that of the bulk:  $H_{c2}^{(\infty)}=2H_E-H_A$ . This is so because, in a finite structure, the surface spins experience weaker exchange fields opposing alignment, as noted above.

For  $N$  even, as we have seen, the situation is more complicated: At low fields, in the antiferromagnetic ground state, if spin  $l=1$  is aligned with the external field, necessarily the  $N$ th spin is in the opposite direction to the

external field. We thus realize the surface spin-flop transition, at a critical field  $H_s$  well below  $H_{c1}$ . Our numerical studies show, as noted in brief remarks on the finite superlattice by Keffer and Chow, that the surface spin rotates nearly  $180^\circ$ , at fields just above the surface spin-flop field. There is a domain wall, initially off center, between two nearly antiferromagnetic regions, just above the surface spin-flop field. With increasing field, the wall "hops" towards the center of the structure, producing spikes in  $dM/dH$ , the derivative of the magnetization with respect to the external field  $H_0$ . Along with its motion, the wall also grows in width with increasing field, and eventually engulfs the entire structure, to produce a continuous transition to the symmetric "bulk" spin-flop state. This is similar to a second-order phase transition. We denote the field at which this occurs as  $H_{c3}$ . This picture has been confirmed by experimental observations.<sup>8</sup> Similarly to the odd- $N$  case, as the field is increased from  $H_{c3}$ , another continuous transition to the ferromagnetic state happens at a field  $H_{c2}$  slightly below that of the infinitely extended superlattice.

These results are summarized in Fig. 3, which appeared also in our earlier publication.<sup>8</sup> For clarity and completeness, we repeat it here. In Fig. 3(a), we show the magnetization as a function of external magnetic field, for the case where the external field is parallel to the easy axis. This is done for a superlattice with 15 ferromagnetic films, and also for a superlattice with 16 films. The parameters are  $H_E = 2.0$  kG, and  $H_A = 0.5$  kG. These appear to describe the samples used in Ref. 8.

The magnetization curve for  $N = 15$  shows the "bulk" spin-flop transition just below 1.5 kG; there is a discontinuous jump in magnetization here (first-order phase

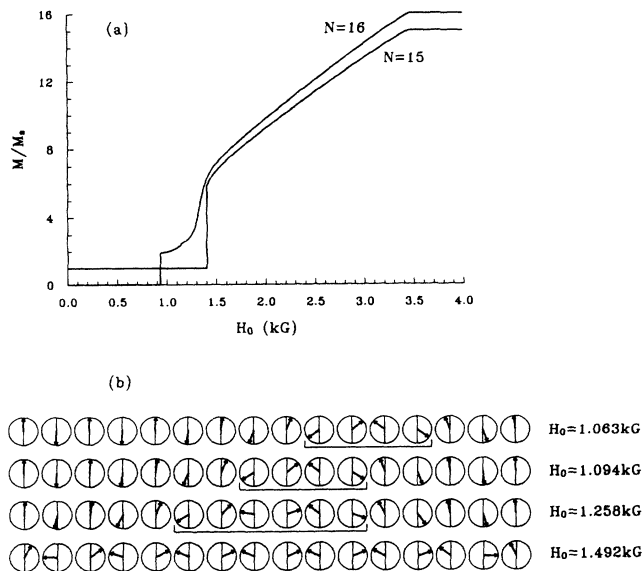


FIG. 3. (a) Total magnetic moment, as a function of external magnetic field, for (i) a 15-unit cell, and (ii) a 16-unit cell of a model Fe/Cr(211) superlattice. (b) For the 16-layer superlattice, we show the arrangement of ferromagnetic moments, for various applied fields.

transition). For the infinitely extended superlattice, in the spin-flop phase, the magnetization is strictly linear in external field, for the present model. There is clear curvature in the curve labeled  $N = 15$ . This is most evident just above the bulk spin-flop field, in Fig. 3(a). The curvature has its origin in surface effects.

The curve for  $N = 16$  is very different than that for  $N = 15$ . We see a jump discontinuity in the magnetization near 0.9 kG, at a field roughly  $\sqrt{2}$  smaller than  $H_{c1}$ , in agreement with the early discussions<sup>3,4</sup> (which centered on the limit  $H_A \ll H_E$ ). Notice that the magnetization curve is *continuous* in the near vicinity of  $H_{c3}$ . This is because, as argued by Keffer and Chow, the surface spin-flop state evolves into the bulk spin-flop state in a continuous manner.

This evolution is illustrated in Fig. 3(b). The spin arrangement labeled  $H_0 = 1.063$  kG is that realized a bit below the surface spin-flop transition. We can view the structure as one with a domain wall separating two nearly antiferromagnetic regions; the moment of the film on the right end of the structure (antiparallel to the external field in the low-field state) rotates by an angle very close to  $180^\circ$  at the surface spin-flop field.

With increasing field, there are *discontinuous* jumps of the domain wall towards the center of the structure. The spin array labeled  $H_0 = 1.094$  kG shows the configuration after one such jump. The domain wall migrates to the center of the structure (spin configuration labeled  $H_0 = 1.258$  kG), and broadens as the magnetic field increases. The bulk spin-flop arrangement, with end effects noted earlier, evolves out of this configuration (configuration labeled  $H_0 = 1.492$  kG).

The discontinuous domain wall jumps leave their signature on the magnetization curves, though this is difficult to perceive in Fig. 3(a). We see these effects more clearly in  $dM/dH$ , the derivative of magnetization with respect to field. In Fig. 4(a), taken also from Ref. 8, we show  $dM/dH$  for  $N = 15$ . The sharp spike, in reality a  $\delta$  function for our model, marks the onset of the bulk spin-flop transition. In Fig. 4(b), we give  $dM/dH$  for  $N = 16$ . We see a sequence of spikes within the surface spin-flop regime. These spikes are introduced by the domain wall jumps. There is a very sharp cusp in  $dM/dH$  at  $H_{c3}$ , but as remarked earlier the magnetization is continuous here.

Experimental studies at Argonne National Laboratory for superlattices with  $N = 20$  and 21 provide  $dM/dH$  curves in excellent accord with the above analysis, though the data do not resolve the spikes introduced by the domain wall jumps. Studies of the magnetization via the magneto-optic Kerr effect reveal that the surface spin flop is indeed localized near one surface of the structure. A discussion of these results is presented elsewhere.<sup>8</sup>

The "bulk" spin-flop transition for the case where we have an odd number of layers is a first-order magnetic-field-induced phase transition. The same is true for the surface spin-flop state in the even case. We thus expect hysteresis effects in the vicinity of the phase-transition fields. The magnetization curves displayed above are all calculated by finding the absolute minimum value of the energy for each field. If, for example, we start with the low-field antiferromagnetic state and increase the exter-

nal field, the spin arrangement will remain *locally* stable, i.e., stable with respect to small-amplitude spin fluctuations, up to magnetic fields higher than that where the energy of the low-field state crosses that of a flopped configuration. Similarly, if we start with high fields and

decrease the field, a spin-flop state will be locally stable until a field below the energy crossing is reached.

We may construct a stability diagram and probe the dynamical stability of a given state by studying the eigenvalues of the matrix

$$\begin{aligned}
 M_{ij} &\equiv \partial^2 E / \partial \alpha_i \partial \alpha_j \\
 &= -\frac{H_E}{2} \cos(\alpha_i + \alpha_j) (1 - \delta_{i,1}) / \delta_{i,j+1} - \frac{H_E}{2} \cos(\alpha_i + \alpha_j) (1 - \delta_{i,N}) \delta_{i,j-1} \\
 &\quad + \left\{ H_0 \cos \alpha_i + H_A \cos 2\alpha_i - \frac{H_E}{2} [\cos(\alpha_i + \alpha_{i-1}) (1 - \delta_{i,1}) + \cos(\alpha_i + \alpha_{i+1}) (1 - \delta_{i,N})] \right\} \delta_{i,j}, \quad (3)
 \end{aligned}$$

where  $i, j = 1, \dots, N$ . All eigenvalues of the matrix  $\mathbf{M}$  must be positive for the state to be stable.

Note that it is clear that stability may be explored by varying only the direction of magnetization of the various films, keeping them always in plane. If we tilt the magnetization of a given film out of plane, an internal demagnetizing field antiparallel to the out-of-plane component of the magnetization will be generated, and this will clearly increase the energy of the state above that associ-

ated with tilting the magnetization in plane through the same angle.

In constructing a stability diagram, we start from a stable equilibrium configuration, and increase or decrease the external magnetic field until it ceases to be in stable equilibrium. In this fashion, we construct the stability diagrams given in Fig. 5, for  $N = 15$  and  $N = 16$  layers. The arrows indicate the path taken by the sample, if with either increasing or decreasing field the material remains

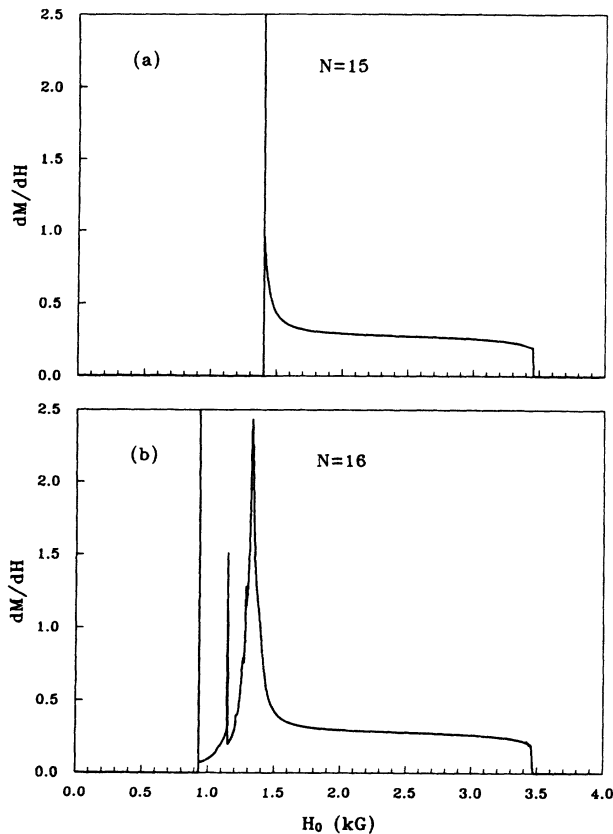


FIG. 4. Plots of  $dM/dH$  for (a) the 15-layer structure whose magnetic moment is described in Fig. 3(a), and (b) the 16-layer structure whose magnetic moment is described in Fig. 3(b). The spikes in the surface spin-flop region are introduced by domain wall jumps.

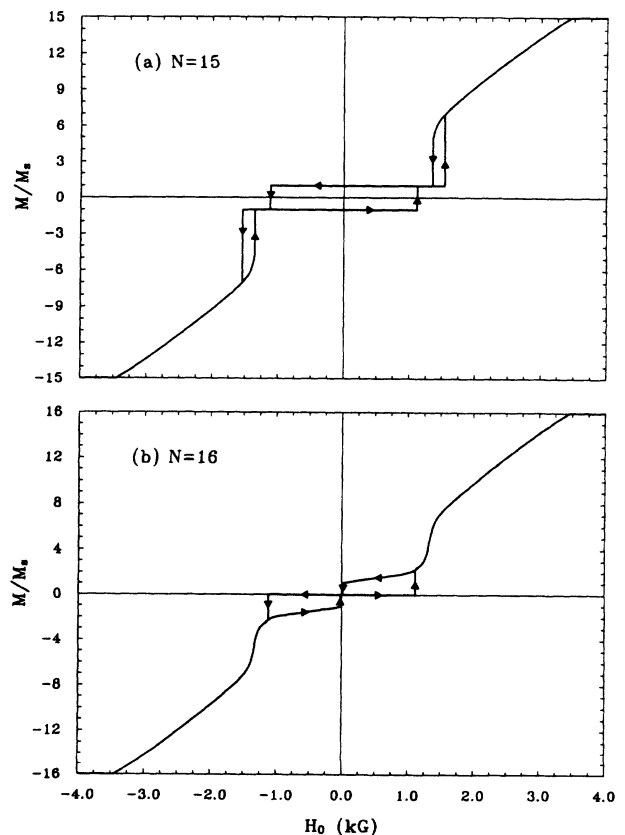


FIG. 5. Stability diagrams, illustrating the limits of stability for superlattices with an even and an odd number of layers, respectively. We show stability diagrams for the cases (a)  $N = 15$  and (b)  $N = 16$  layers.

in a given configuration throughout switching, passing the point where its energy crosses that of a different phase, until the absolute stability limit is reached. These diagrams can be viewed as model hysteresis loops, provided the system indeed makes full excursions of the sort just described.

Comments are necessary to describe how these diagrams are constructed. Several different phases are found, as we now illustrate for the case where  $N$  is even. We can begin with the low-field antiferromagnetic state, whose energy is independent of the field  $H_0$ . It is straightforward to increase  $H_0$ , until the stability threshold is reached, by the criterion given above. Similarly, one may begin with the high-field ferromagnetically aligned state with  $H_0$  large, decrease  $H_0$ , and find the stability limit of the phase, keeping all moments aligned ferromagnetically. When this is done, at a field just a very tiny amount higher than the stability limit of the saturated state, we find a symmetric state splits off, to fall lower in energy. In the symmetric state, which is the configuration we identify as the bulk spin-flop state, we have  $\alpha_l \equiv \alpha_{N+1-l}$ . Note that the remarks just made imply the presence of hysteretic behavior in the vicinity of the field where, with increasing field, the system saturates. This effect leads to a very tiny loop, too small to show in Fig. 5. We believe this to be a finite-size effect, which vanishes as  $N \rightarrow \infty$ , and which is too small to observe.

We may explore the stability limit of the symmetric bulk spin-flop state with the above criterion employed, and the constraint  $\alpha_l \equiv \alpha_{N+1-l}$  imposed as the field is lowered. The surface spin-flop configuration is asymmetric as one sees from Fig. 3(b). A description of this phase is generated by removing the constraint  $\alpha_l \equiv \alpha_{N+1-l}$ ; we find the asymmetric solution at lower fields, and with increasing field its energy merges with that of the symmetric state. Once one "locks onto" the asymmetric state, its stability is again explored through use of the same criterion. With decreasing field, the asymmetric state becomes unstable at a very small but nonzero field, for the example considered. This is difficult to appreciate from Fig. 5(b).

This summarizes our studies of the magnetic phase diagrams of our model of the Fe/Cr(211) superlattice. We have considered samples with fewer ferromagnetic films; we shall not present the details of the studies here. The calculations reported above are demanding from the perspective of numerical precision. As a consequence, we have found it difficult and time consuming to explore values of  $N$  greater than 16.

We turn next to an examination of the collective spin-wave modes of the superlattices.

### III. COLLECTIVE SPIN-WAVE MODES OF THE SUPERLATTICE

We discuss in this section the collective spin-wave modes of the superlattice structure, in the various magnetic-field-induced phases described in Sec. II. Before we turn to the details of the present treatment, some general discussions will be useful.

#### A. General remarks

Our attention here will be confined to the limit where the ferromagnetic film can be regarded as very thin. We suppose the spins within a given film are linked together by very strong intrafilm exchange, so when a spin wave is excited, the precessing component of the magnetization within a given film is uniform across the film. That is, in film  $l$ , let  $\mathbf{m}(l; \mathbf{x}; t)$  be the fluctuating component of the magnetization when a spin wave is excited. Quite generally, with  $y$  the axis normal to the film surface (the easy axis here is always in plane, and in the  $\hat{z}$  direction, as in Fig. 2), we have

$$\mathbf{m}(l; \mathbf{x}; t) = \mathbf{m}(l; y) \exp(ik_x x + ik_z z - i\omega t)$$

when a spin wave is excited. The thin-film limit we invoke supposes  $\mathbf{m}(l; y)$  to be independent of  $y$ . This approximation is valid so long as we consider films whose thickness is thin compared to  $(D/\omega)^{1/2}$ , with  $D$  the spin-wave exchange stiffness, and  $\omega$  a typical spin-wave frequency. For Fe, this approximation is quite adequate until the film thickness reaches the 100 Å range.

The mathematics becomes quite complex when this approximation breaks down, as demonstrated by early discussions of the influence of exchange on the spin waves excited near the surface of ferromagnets, and in thin ferromagnetic films.<sup>12,13</sup> An extension of this formalism to superlattices would lead to calculations of formidable technical complexity. The approximation just described, combined with our simple treatment of the interfilm dipolar couplings, leads to a rather straightforwardly implemented formalism.

Collective spin-wave excitations of the entire superlattice structure result because the spin waves in the various ferromagnetic films interact through two mechanisms. One is the interfilm exchange, and the other is the interfilm dipolar interactions of long range, with origin in magnetic fields generated by the precessing magnetic moments.

The exchange couplings are the same which enter our analysis of the magnetization curves. Our analyses of the magnetization curves did not require the inclusion of dipolar effects, because, as noted above, the magnetization always lies in the plane; no demagnetizing fields are generated by reorientation of the magnetization so long as the films are infinite in extent. This is the reason why there is close correspondence between the analysis in Sec. II and the very early discussions of the surface spin-flop transition,<sup>4,6</sup> which also ignored dipolar effects.

It was noted that Saslow and Mills<sup>3</sup> found a "soft" surface spin wave to be associated with the surface spin-flop transition. Their analysis of the spin dynamics ignored dipolar effects also; this is surely reasonable for the antiferromagnetic crystals of interest to them, within which the exchange fields are larger than dipole fields by perhaps two orders of magnitude. The parameters which characterize the Fe/Cr(211) superlattices fall in a very different regime. We have seen that Argonne Laboratory samples are characterized, in the language of Eq. (1), by  $H_E \cong 2.0$  kG and  $H_A \cong 0.5$  kG. A measure of the influence of dipolar fields is given by  $4\pi M_s$ , which in Fe

is 21 kG. Thus, in the superlattices of interest, the dipolar fields are very much *larger* than the exchange. Dipolar fields are generated when spin waves are excited, by virtue of the elliptical polarization of the modes, which necessarily generates a component of magnetization normal to the surface, and also by the resulting spatial modulation of the magnetization. The spin dynamics of the superlattice structure will thus differ qualitatively from that in the analysis of Saslow and Mills.

We shall consider spin waves with wavelength long compared to a lattice constant in the present paper. The dipolar effects can then be described macroscopically. There are two distinct effects, which are illustrated by considering a single, isolated film. Consider first a spin wave with wave vector  $k_{\parallel}=0$ , the uniform mode of the film. As the magnetization precesses, an internal demagnetizing field is generated, of strength  $-4\pi m_y(l)\hat{y}$ , by the component of the precessing magnetization normal to the film surfaces. It is this field which upshifts the resonance of the film from the value  $\gamma H_0$  to  $\gamma[H_0(H_0+4\pi M_s)]^{1/2}$ . This effect has been well understood for many decades.<sup>14</sup> When  $k_{\parallel}=0$ , within macroscopic theory, the demagnetizing field is confined entirely to within the film; there are no interfilm dipolar couplings in a multifold superlattice in this limit.

Now when  $k_{\parallel}$  is nonzero, though the wavelength is still long compared to a lattice constant, one encounters a new effect. The dipolar fields generated by the spin precession in a given film are no longer confined to the film, but instead they leak out. In the superlattice, we then have interfilm couplings of dipolar origin. In our thin-film limit, we shall always be assuming  $k_{\parallel}d \ll 1$ , where  $d$  is the film thickness. Then the dipolar fields outside a single film with static magnetization parallel to  $\hat{z}$  are easily shown to have components (in the region  $y > d/2$ )

$$h_y^{(d)} = 2\pi k_{\parallel} d \left[ m_y - i \frac{k_x}{k_{\parallel}} m_x \right] \exp[-k_{\parallel}(y-d/2)], \quad (4a)$$

$$h_x^{(d)} = 2\pi k_x d \left[ m_y + i \frac{k_x}{k_{\parallel}} m_x \right] \exp[-k_{\parallel}(y-d/2)], \quad (4b)$$

$$h_z^{(d)} = 2\pi k_z d \left[ m_y + i \frac{k_x}{k_{\parallel}} m_x \right] \exp[-k_{\parallel}(y-d/2)], \quad (4c)$$

where  $m_x$  and  $m_y$  are here assumed very small. We omit the trivial factors  $\exp(ik_x x + ik_z z - i\omega t)$  from these expressions. It is assumed that the film lies between  $y = -d/2$  and  $y = d/2$ .

A measure of the strength of the interfilm dipolar coupling, noting it to be rather long range, is  $4\pi M_s k_{\parallel} d N_d$ , with  $N_d$  the number of films which are linked by the fields displayed in Eqs. (4). There are then two cases for the finite superlattices explored here. The first is the regime  $k_{\parallel}D \gtrsim 1$ , with  $D$  the superlattice thickness. Then a rough estimate of  $N_d$  is  $N_d \approx 1/k_{\parallel}d$ , and the influence of the interfilm dipolar couplings is very large indeed, comparable to that of the internal demagnetizing field which shifts the uniform mode frequency from  $\gamma H_0$  to  $\gamma[H_0(H_0+4\pi M_s)]^{1/2}$ . In this regime, the collective excitations of the superlattice are very different in character

from analyses such as that presented by Saslow and Mills. The calculations reported below show, for example, that in this regime there is no hint of their soft mode.

Now in the regime  $k_{\parallel}D \ll 1, N_d = N$ , the total number of films in the lattice. A measure of the role of interfilm dipolar coupling is provided by  $4\pi M_s k_{\parallel} D$ , which for  $k_{\parallel}D \ll 1$  can be small compared to both  $H_E$  and  $H_A$ . The internal, intrafilm demagnetizing field remains always, of course. We find below that the spin dynamics which emerges when  $k_{\parallel}D \ll 1$  is very similar to that discussed by Saslow and Mills: there is a "soft" surface spin-wave mode, whose frequency vanishes as the stability limit of the low-field antiferromagnetic state is approached from below, with increasing external field  $H_0$ .

There are important experimental implications of these remarks. The spin waves excited in light-scattering experiments typically have wave vectors in the range of  $10^5 \text{ cm}^{-1}$ , and for the Argonne samples this places one in the regime  $k_{\parallel}D \gtrsim 1$ . We are in the regime where interfilm dipolar couplings play a central role. On the other hand, microwave resonance excites collective modes with  $k_{\parallel}D \ll 1$ . This technique should allow study of the low-frequency mode which softens as an external magnetic field drives the system towards the surface spin-flop. These points will be illustrated by the calculations presented below.

## B. The formalism

We begin the discussion of the collective spin-wave excitations as follows. We suppose the  $l$ th film has a magnetization we write

$$\mathbf{M}(l; \mathbf{x}; t) = \mathbf{M}_0(l) + \mathbf{m}(l; \mathbf{x}; t),$$

where, following the remarks above, the time-dependent portion is written

$$\mathbf{m}(l; \mathbf{x}; t) = \mathbf{m}(l) \exp(ik_x x + ik_z z - i\omega t),$$

in the limit where the spins in film  $l$  are rigidly locked together by strong intrafilm exchange. Here  $\mathbf{M}_0(l)$  is the static magnetization, whose orientation is found from calculations such as those in Sec. II. The basic equation of motion is

$$\frac{d}{dt} \mathbf{M}(l; \mathbf{x}; t) = \gamma \mathbf{H}_{\text{eff}}(l) \times \mathbf{M}(l; \mathbf{x}; t). \quad (5)$$

We shall linearize this equation with respect to  $\mathbf{m}$ .

The quantity  $\mathbf{H}_{\text{eff}}(l)$  is the effective field which acts on film  $l$ . It consists of several pieces. One has, of course, the external Zeeman field  $\hat{z}H_0$ . The anisotropy energy adds a contribution which we write  $\hat{z}M_z(l; \mathbf{x}; t)/M_s$ , with  $M_s$  the saturation magnetization. There is then the interfilm exchange, followed by the dipolar contribution  $\mathbf{H}_d(l)$ . Thus we have

$$\begin{aligned} \mathbf{H}_{\text{eff}}(l) = & \hat{z}H_0 + \hat{z} \frac{H_A}{M_s} M_s(l; \mathbf{x}; t) \\ & - \frac{H_E}{2M_s} [\mathbf{M}(l-1; \mathbf{x}; t)(1-\delta_{l,1}) \\ & + \mathbf{M}(l+1; \mathbf{x}; t)(1-\delta_{l,N})] + \mathbf{H}_d(l). \quad (6) \end{aligned}$$

Our means of generating the dipolar field requires some discussion. In the case of very thin films, we could simply follow Nörtemann *et al.*<sup>10</sup> and evaluate the relevant dipole sums in a microscopic manner, using techniques introduced earlier.<sup>15</sup> Here we introduce a macroscopic approach, which captures the essential key aspects, in the thin-film limit.

The dipolar fields generated by the spin motions can, in the magnetostatic limit, be written as the gradient of a scalar potential. We suppose for the moment that the dipole field  $\mathbf{H}_d$  is a continuous function of  $\mathbf{x}$  and  $t$ , and then make contact with the quantity  $\mathbf{H}_d(l)$  in Eq. (6) later. Thus

$$\mathbf{H}_d(\mathbf{x};t) = -\nabla\varphi(\mathbf{x};t), \quad (7)$$

where, of course,

$$\varphi(\mathbf{x};t) = \Phi(y)\exp(ik_x x + ik_z z - i\omega t). \quad (8)$$

Inside film  $l$ , where  $\mathbf{m}$  is viewed as independent of  $y$ , one has, with  $k_{\parallel}^2 = k_x^2 + k_z^2$ ,

$$\left[ \frac{d^2}{dy^2} - k_{\parallel}^2 \right] \Phi(y) - 4\pi i [k_x m_x(l) + k_z m_z(l)] = 0. \quad (9)$$

The most general solution of Eq. (9) can be written as

$$\begin{aligned} \Phi(y) = & A_{l,l} \cosh k_{\parallel} [y - (l-1)d] \\ & + B_{l,l} \sinh k_{\parallel} [y - (l-1)d] \\ & - \frac{4\pi i}{k_{\parallel}^2} [k_x m_x(l) + k_z m_z(l)]. \end{aligned} \quad (10a)$$

The geometry is as follows. The superlattice unit cell has thickness  $d$ , and  $d_1 < d$  is the thickness of the ferromagnetic films. Then film  $l$  is taken to occupy the region  $(l-1)d \leq y < (l-1)d + d_1$ . The nonmagnetic spacers have thickness  $d_2$ , so that  $d = d_1 + d_2$ .

The expression in Eq. (10a) describes the magnetic potential within film  $l$ . We need this same quantity in the regions between the films, and we then link the various coefficients through boundary conditions. Just above film  $l$ , in the region  $(l-1)d + d_1 \leq y < ld$ , we write

$$\begin{aligned} \Phi(y) = & A_{l,l+1} \cosh k_{\parallel} [y - d_1 - (l-1)d] \\ & + B_{l,l+1} \sinh k_{\parallel} [y - d_1 - (l-1)d], \end{aligned} \quad (10b)$$

and just below the film, in the region  $(l-1)d - d_2 \leq y < (l-1)d$ , we have

$$\begin{aligned} \Phi(y) = & A_{l-1,l} \cosh k_{\parallel} [y + d_2 - (l-1)d] \\ & + B_{l-1,l} \sinh k_{\parallel} [y + d_2 - (l-1)d]. \end{aligned} \quad (10c)$$

The boundary conditions at each interface are to require the continuity of  $\Phi(y)$ . This ensures continuity of the tangential components of the dipole field. Then normal components of  $\mathbf{B}$  are conserved; within the film  $B_y = -d\Phi/dy + 4\pi m_y$ . The boundary conditions applied to the surfaces of film  $l$  then lead to a set of inhomogeneous equations which link the various coefficients together:

$$\begin{aligned} A_{l,l} \cosh k_{\parallel} d_1 + B_{l,l} \sinh k_{\parallel} d_1 - A_{l,l+1} \\ = \frac{4\pi i}{k_{\parallel}^2} [k_x m_x(l) + k_z m_z(l)], \end{aligned} \quad (11a)$$

$$A_{l,l} \sinh k_{\parallel} d_1 + B_{l,l} \cosh k_{\parallel} d_1 - B_{l,l+1} = \frac{4\pi}{k_{\parallel}} m_y(l), \quad (11b)$$

$$\begin{aligned} A_{l-1,l} \cosh k_{\parallel} d_2 + B_{l-1,l} \sinh k_{\parallel} d_2 - A_{l,l} \\ = -\frac{4\pi i}{k_{\parallel}^2} [k_x m_x(l) + k_z m_z(l)], \end{aligned} \quad (11c)$$

and

$$A_{l-1,l} \sinh k_{\parallel} d_2 + B_{l-1,l} \cosh k_{\parallel} d_2 - B_{l,l} = -\frac{4\pi}{k_{\parallel}} m_y(l). \quad (11d)$$

These relations apply formally to all the films,  $l=1, \dots, N$ . In addition, the outermost surface of each of the end films is matched to a scalar potential that falls to zero exponentially with increasing distance from the structure, as  $\exp(\pm k_{\parallel} y)$ . Let the superlattice structure extend from  $y=0$  to  $y=D$ . Then for  $y < 0$ , we write the potential as  $\Phi(y) = c_{<} \exp k_{\parallel} y$ , while for  $y > D$ , we have  $\Phi(y) = c_{>} \exp[-k_{\parallel}(y-D)]$ . Using the above procedure, we match the solutions at the outermost surface.

We are then led to a set of  $4N+2$  inhomogeneous equations in the coefficients  $A_{l,l}, B_{l,l}$ , etc. combined with  $c_{<}$  and  $c_{>}$ . It is a simple matter of matrix inversion to find a relation of the form

$$\begin{aligned} A_{l,l} = & \sum_{l'} \Gamma^{(x)}(l, l') m_x(l') + \sum_{l'} \Gamma^{(y)}(l, l') m_y(l') \\ & + \sum_{l'} \Gamma^{(z)}(l, l') m_z(l'), \end{aligned} \quad (12)$$

and similarly for  $B_{l,l}$ .

The dipolar field inside film  $l$  has in the general case a dependence on  $y$ . In the thin-film limit that  $\mathbf{m}$  is regarded as independent of  $y$ , the spins sense only the *average* field within the film. Thus, after carrying out the averaging procedure, we generate an expression for the field  $\mathbf{H}_d(l)$  which enters Eq. (6). When  $k_{\parallel} d_1 \ll 1$ , this relation takes the form

$$\mathbf{H}_d(l) = -i\mathbf{k}_{\parallel} A_{l,l} - \hat{y} k_{\parallel} B_{l,l} - \frac{4\pi \mathbf{k}_{\parallel}}{k_{\parallel}^2} \left[ \mathbf{k}_{\parallel} \cdot \mathbf{m} \right]. \quad (13)$$

If one works entirely in a laboratory coordinate system, then by this method one obtains a  $3N \times 3N$  matrix to diagonalize. In this matrix,  $N$  eigenvalues are identically zero,  $N$  are positive numbers, and  $N$  are negative numbers. The  $2N$  nonzero eigenvalues are the physical spin-wave frequencies. The negative eigenvalues correspond to waves which propagate across the structure in the opposite sense to the positive set. Thus, if one compares the set with a particular choice of  $\mathbf{k}_{\parallel}$  with those generated by the choice  $-\mathbf{k}_{\parallel}$ , the positive- and negative-frequency set are interchanged.

If one desires, one can reduce the size of the eigenvalue problem to that of a  $2N \times 2N$  matrix. This is done by

erecting a local coordinate system in each film, with a local  $z$  axis aligned along the magnetization. The two components perpendicular to the magnetization only then enter the discussion, and all  $2N \times 2N$  eigenvalues are nonzero. Since  $N$  is not very large in the examples considered here, we saw little motivation to do this.

### C. Calculations of the collective spin-wave modes of the structure

We now turn to the results of our studies of the collective modes of the finite Fe/Cr structures. We shall concentrate on the case where we have an even number of layers, and the surface spin-flop transition thus develops.

In Fig. 6, we show the frequencies of the collective spin-wave modes of the structure with 16 layers, whose magnetization curve is illustrated in Fig. 3(a). For these calculations, we have chosen  $k_{\parallel}d=0.05$ , with  $d$  the thickness of the unit cell, which is 51 Å for the structure considered. Notice this means  $k_{\parallel}D=0.8$ , where  $D$  is the thickness of the entire structure. We are thus in the regime where, according to our earlier discussions, the spin-wave spectrum of each film is influenced strongly by interfilm dipolar interactions. We show both positive- and negative-frequency eigenvalues.

First consider the low-field antiferromagnetic state, which occupies the field region  $H_0 < 0.9$  kG. The first thing one notices is that we have a very high-frequency mode, split off from the various other normal modes of the structure. This mode can be viewed as the uniform mode of the entire structure. For this mode, the component of precessing magnetization parallel to the surface,  $m_x$ , has the same sign in each film, with magnitude that varies modestly through the stack of Fe films. On the other hand,  $m_y$  oscillates in sign. One can appreciate that, for a system with antiferromagnetic ground state,

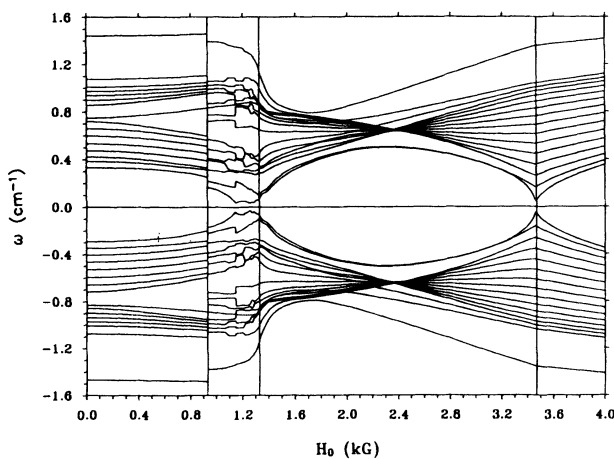


FIG. 6. Magnetic-field dependence of the spin-wave spectrum of the 16-layer superlattice where magnetization curve is given in Fig. 3(a). The calculations assume  $k_{\parallel}d=0.05$ , with  $d$  the thickness of the unit cell. The propagation direction is perpendicular to the external magnetic field. Also, we have assumed  $4\pi M_s=21$  kG for each film. Each Fe film contains 25 atomic layers, and each Cr film contains eight atomic layers.

this eigenmode generates a dipolar field which couples strongly to the spin motion, through the  $M_z H_y$  and  $M_z H_x$  terms in the equation of motion. In the antiferromagnetic state,  $M_z$  alternates in sign as one moves from film to film, so an oscillatory dipolar field generates a coherent torque on the film in the system.

In the low-field state, there are in the spectrum two surface modes of exchange character, one localized to the left surface and one to the right surface. Recall that the rightmost film is antiparallel to the external field. The lowest-frequency mode, for both signs of  $k_{\parallel}$ , is rather highly localized to the right-hand surface, where antiparallel alignment is responsible for the surface spin-flop transition. The ninth mode, which at higher fields can be seen to lie in a gap between “acoustical” and “optical” standing-wave resonances in the structure, is localized to the left-hand surface.

The lowest-frequency mode, the exchange mode localized to the right surface, can be recognized as the analog of the soft mode discussed in the early literature as the surface spin-flop transition.<sup>3,4</sup> We see that, as the surface flop field is approached from below (this is indicated by the vertical line near 0.9 kG), this mode softens only very slightly. Dipolar stiffening, in this regime of wave vector, suppresses the soft-mode behavior.

The surface spin-flop region lies between the vertical lines just above  $H_0=0.9$  kG and  $H_0=1.3$  kG. As the field increases, one sees discontinuous jumps in the frequencies of the various modes. The discontinuities arise from the field-induced domain wall jumps discussed earlier.

We enter the symmetric bulk spin-flop state just above an applied field of 1.3 kG. We see again a high-frequency mode split off from the mode spectrum of the structure. With increasing field, this mode acquires the characteristic of the well-known Damon-Eshbach mode associated with ferromagnetic films. The negative-frequency mode tends to localize on the left surface, and the positive-frequency mode on the right surface. The two nearly degenerate modes of lowest frequency are exchange surface waves, which are symmetric and antisymmetric combinations of eigenvectors localized on the two surfaces.

One can also notice the convergence of spectra at fields around 2.4 kG. This is because the inner spins of the structure are making an angle of nearly  $90^\circ$  with each other, and the effective exchange fields are inoperative.

In the high-field saturated state, the high-frequency mode, split off from the band of standing-wave modes, can be viewed as a uniform mode of the stack of films, where all the film magnetizations precess in phase. Here both  $m_y$  and  $m_x$  are roughly constant across the structure.

This summarizes the nature of the collective modes, in the regime of wave vectors appropriate to Brillouin light studies. We turn to the limit  $k_{\parallel}D \ll 1$  next.

As remarked earlier, when  $k_{\parallel}D \ll 1$ , the interfilm dipolar couplings become negligible, and the dipolar couplings lead only to the intrafilm dynamic demagnetizing field  $-4\pi m_y \hat{y}$ . In this limit, the dispersion in the spin-wave spectrum of the structure is controlled only by the interfilm exchange.

In Fig. 7, we show the magnetic-field dependence of the collective spin-wave spectrum when  $k_{\parallel}=0$ . One notices that the very high-frequency mode presented in Fig. 6 is missing. At each field, the mode was split off from the standing-wave resonances of the structure by the interfilm dipolar couplings, which are now absent. Further evidence of their absence is provided by the fact that the negative-frequency eigenvalues are equal and opposite to the positive-frequency ones. The nonreciprocity induced by the interfilm dipolar coupling is now absent.

In the low-field state, the eigenvalues cluster into an optical spin-wave branch, and an acoustical spin-wave branch. This is most evident at the higher fields. In the regime where, for example,  $H_0 \sim 0.5$  kG, the highest seven modes are standing resonances of optical magnon character. The next mode down, which lies in the gap between the optical and acoustical cluster, is an exchange-dominated surface mode, localized near the left surface, where film magnetization is parallel to the external field. Modes 9–15 (counting down from the top) are standing waves of acoustical character.

The lowest-frequency mode is also an exchange surface mode, as before, localized at the surface whose film is antiparallel to the external field. This mode softens more substantially than its counterparts in Fig. 6 as the surface spin-flop field is approached from below, since the “stiffening” provided by interfilm dipolar interaction is now absent. We have followed the frequency of this mode as the external field is increased beyond the surface spin-flop field, to the point where the low-field ground state becomes unstable (see the model hysteresis curve in Fig. 5). The frequency of the mode vanishes as the stability limit is approached from below. This lowest mode is thus the equivalent of the “soft mode” found earlier by Saslow and Mills.<sup>3</sup>

We have, in both Fig. 6 and Fig. 7, a mode that very nearly goes soft, as the saturation field is approached from either above or below (see near 3.5 kG). In the bulk two-sublattice antiferromagnet, with dipolar couplings ignored, one has a true soft mode at this field, which is a second-order phase transition. We see that in the finite superlattice the mode frequency remains finite. This is a size effect. We also find a very small degree of hysteresis in the transition from the bulk spin-flop to the saturated state, though this is too small to illustrate in Fig. 5.

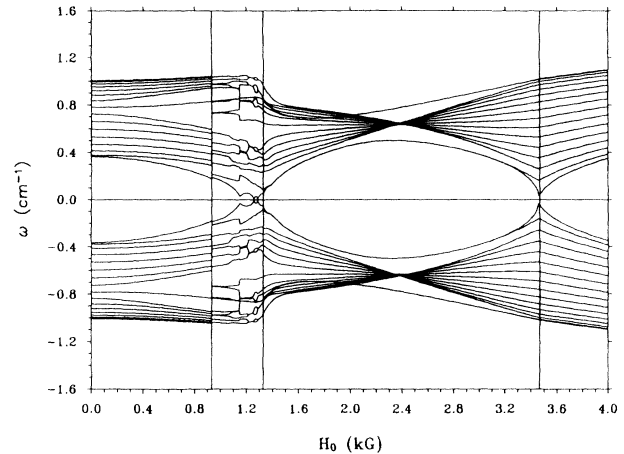


FIG. 7. Same as in Fig. 6, except now we have taken  $k_{\parallel}=0$ .

#### IV. CONCLUDING REMARKS AND DISCUSSIONS

This paper has discussed both the magnetization curves and the dynamic response characteristics of Fe/Cr(211) superlattices grown on MgO(110). The results suggest that it would be of great interest to compare the response characteristics as probed by Brillouin scattering studies with those in the microwave regime. In the former case, we are examining collective modes with wave vectors  $k_{\parallel}$  in the range of  $10^5$   $\text{cm}^{-1}$ , while in the latter we have  $k_{\parallel} \cong 0$ . Thus, for reasons we have discussed, interfilm dipolar interactions influence the modes probed by light scattering, but their influence will be quite negligible in the microwave region.

It is our understanding that, at present, light-scattering studies of the Fe/Cr(211) structures are under way.<sup>16</sup> We are presently generating theoretical descriptions of the spectra. These results, along with a comparison with the data, will be discussed elsewhere.

The studies presented here show that the Fe/Cr(211) superlattices are rich systems, and we hope the calculations will stimulate further experimental study.

#### ACKNOWLEDGMENTS

We have enjoyed stimulating discussions with Dr. E. Fullerton, Dr. M. Grimsditch, and Sudha Kumar. This research was supported by the Army Research Office, under Contract No. CS001028.

<sup>1</sup>M. N. Baibich, J. M. Broto, A. Fert, F. Nguyen Van Dau, F. Petroff, P. Eitenne, G. Creuzet, A. Freyciderich, and J. Chazeles, *Phys. Rev. Lett.* **61**, 2472 (1988).

<sup>2</sup>Eric E. Fullerton, M. J. Conover, J. E. Mattson, C. H. Sowers, and S. D. Bader, *Phys. Rev. B* **48**, 15 755 (1993).

<sup>3</sup>W. Saslow and D. L. Mills, *Phys. Rev.* **171**, 488 (1968).

<sup>4</sup>D. L. Mills, *Phys. Rev. Lett.* **20**, 18 (1968).

<sup>5</sup>S. Foner, in *Magnetism*, edited by G. Rado and H. Suhl (Academic, New York, 1966), p. 384.

<sup>6</sup>F. Keffer and H. Chow, *Phys. Rev. Lett.* **31**, 1061 (1973).

<sup>7</sup>W. E. Tennant, R. B. Bailey, and P. L. Richards, in *Magnetism and Magnetic Materials*, Proceedings of the 30th Annual

Conference on Magnetism and Magnetic Materials, San Francisco, 1974, edited by C. D. Graham, G. H. Lander, and J. J. Rhyne, AIP Conf. Proc. No. 24 (AIP, New York, 1975).

<sup>8</sup>R. W. Wang, D. L. Mills, Eric E. Fullerton, J. E. Mattson, and S. D. Bader, *Phys. Rev. Lett.* **72**, 920 (1994).

<sup>9</sup>A macroscopic description of interfilm dipolar couplings in superlattice spin-wave spectra was given by R. E. Camley, T. S. Rahman, and D. L. Mills, *Phys. Rev. B* **23**, 1226 (1981), while a recent microscopic formulation has been presented by F. C. Nörtemann, R. L. Stamps, and R. E. Camley, *Phys. Rev. B* **47**, 11 910 (1993).

<sup>10</sup>F. C. Nörtemann, R. L. Stamps, A. S. Carrico, and R. E.

